Bulk Water Modeling

DOI: 10.1002/anie.201203568

Proton Defect Solvation and Dynamics in Aqueous Acid and Base**

*Seyit Kale and Judith Herzfeld**

Our current understanding of proton defects in bulk water depends heavily on the interplay between scattering experiments and ab initio simulations, both of which require such high ion concentrations that the solvation shells overlap and counterion effects become significant. Herein, we overcome these limitations by using LEWIS, an intuitive new model of reactive and polarizable water that enables the simulation of a statistically reliable number of proton hopping events in aqueous acid and base at concentrations of practical interest (0.1M). LEWIS predicts radial distribution functions (RDFs) that are similar to those obtained by density functional theory (DFT) and relative diffusion rates for excess protons and proton holes that compare well with experiment. The simulations show that proton transfers occur primarily between persistent special pairs, a Zundel-type species in the case of an excess proton and its analogue in the case of a proton hole. The simulations also show that, relative to vehicular diffusion, proton transfers contribute more significantly to total defect diffusion in acid than in base.

The currently accepted view of a solvated excess proton involves the coexistence of limiting "Eigen" ($H_3O^+ \cdot (H_2O)_3$) and "Zundel" ($H_5O_2^+$) species (Figure 1A and B).[1] In contrast, the proton hole analogues of these species ($OH^- \cdot (H_2O)_3$ in Figure 1C and $H_3O_2^-$ in Figure 1D) have been controversial. The two Zundel-type species differ in that the hydrogen bond of $H_5O_2^+$ exhibits a single well potential, which is conducive to proton transfer,[2] while the hydrogen bond of $H_3O_2^-$ exhibits a double well potential, albeit with a small barrier.[3] The most convincing experimental evidence for the Zundel analogue comes from rather recent core-level electron spectroscopy[4] and 2D-FTIR spectroscopy.[5] The controversy concerning the Eigen analogue[6] arises from ab initio molecular dynamics (MD). The density functionals that support Eigen analogues[7] fail to predict the correct experimental trend of diffusion constants,[8] that is, $D_{H_3O^+} > D_{OH^-} > D_{H_2O}$. On the other hand, the density functional that predicts the correct trend of diffusion constants,[8] predicts "dynamical hypercoordination",[9] in which a dominant "proton transfer inactive", fourfold-coordinated hydroxide oxygen (Figure 1E) interconverts occasionally with a "proton transfer active", threefold-coordinated species, in spite of the fact that four-fold coordination is not favored in gas-phase clusters.[10] The situation is further complicated by the fact that none of the simulations reproduces the position of the first solvation shell obtained by SPC/E-based empirical potential structure refinement of neutron scattering data.[11] Last but not least, there are indications that hydroxide solvation depends on concentration,[12] and both scattering experiments and ab initio simulations are restricted to fewer water molecules per defect than is typically of practical interest.

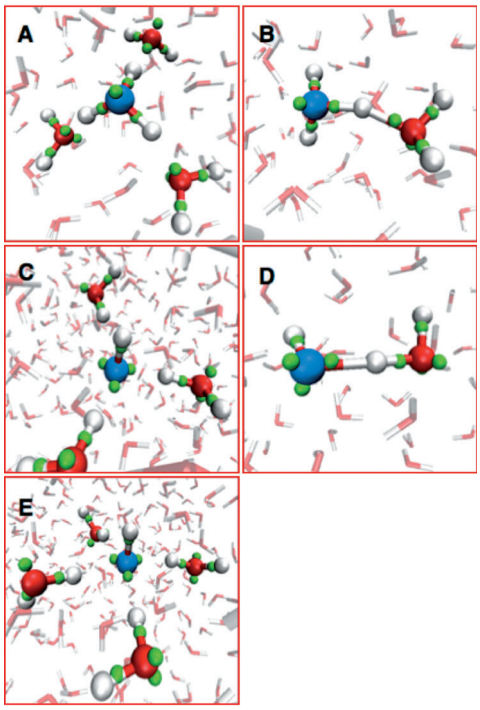

Figure 1. Examples in LEWIS of the limiting solvation forms of proton defects in bulk water. Excess protons in "Eigen" (A) and "Zundel" (B) arrangements, proton holes in analogous arrangements (C and D), and a proton hole accepting four hydrogen bonds (E). The oxygen cores associated with the charge defects are shown in blue instead of red, and the electron pairs are green. Distant water molecules are rendered in stick form. A and C were observed more frequently than B and D, or E.

Empirical methods significantly extend the accessible time- and length-scales of simulations. To perform fully reactive, nanosecond-scale simulations with 500 water molecules we use the amphiprotic and polarizable LEWIS model of water. LEWIS unpacks atoms into their nuclear cores and explicit, interchangeable valence electron pairs, all interacting through carefully designed, pairwise-only potentials.[13] The

[*] Dr. S. Kale
Graduate Program in Biophysics and Structural Biology
Brandeis University
MS 009, 415 South Street, Waltham MA (USA)
Prof.Dr. J. Herzfeld
Department of Chemistry, Brandeis University
MS 015, 415 South Street, Waltham MA (USA)
E-mail: herzfeld@brandeis.edu
Homepage: http://people.brandeis.edu/~herzfeld/

[**] This work was supported by the National Institutes of Health (R01EB001035). Additional computational support was provided by the Brandeis HPC.

Supporting information for this article is available on the WWW under http://dx.doi.org/10.1002/anie.201203568.

mobile electron pairs allow bond formation and breaking, in addition to natural, multidimensional polarizability with the correct geometric response.[14] Thus LEWIS water is both dissociable as in Central Force Model,[15] and polarizable and flexible as in TTM2-F.[16] The training of the LEWIS force field includes intermolecular interactions in the form of neutral, protonated, and deprotonated water dimers. Of particular interest in the present context is the proton hopping barrier in the deprotonated dimer, which is well reproduced by LEWIS, as shown in Figure S1 in the Supporting Information.

For an excess proton, we protonated one water molecule among 500 (corresponding to a pH of ca. 1). Over 10 ns, the proton excess migrated with a diffusion constant of $D_{H_3O^+} = 0.24\ Å^2 ps^{-1}$ (Figure S2) which is ca. 2.2 times the $0.11\ Å^2 ps^{-1}$ value predicted for water (vs. the experimental $D_{H_3O^+}/D_{H_2O}$ ratio of 4.1). By way of comparison (Figure 2), the $D_{H_3O^+}/D_{H_2O}$ value predicted by ab initio MD (for deuterated systems) varies markedly with the choice of density functional, ranging from 10.8 for PW91, to 11.3 for BLYP, to 5.08 for HCTH (vs. the experimental ratio of 3.6 for deuterated systems).[8]

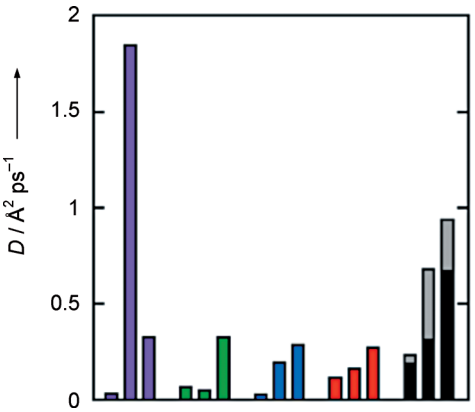

Figure 2. Diffusion rates of water, hydroxide, and hydronium species, respectively, from experiment (^{2}H, ■; ^{1}H, ■) and as predicted by PW91 (^{2}H, ■), HCTH (^{2}H, ■), BLYP (^{2}H, ■), and LEWIS (^{1}H, ■). Of the three common density functionals, PW91, HCTH, and BLYP, only the last predicts the experimentally observed trend of the three diffusion constants.[8] However, the BLYP diffusion constant for water is very small. Experimental data are shown for both ordinary[17] and deuterated[18] species, because the latter is used in DFT simulations for technical convenience.[19]

Structurally, the LEWIS RDFs for hydronium (Figure 3 A) are in reasonable agreement with the empirical potential structure refinement of neutron scattering data,[20] except for a slight overpopulation between the first two shells. This intershell region is underpopulated in empirical MS-EVB, with the best agreement so far observed in MS-EVB3.[2] Among the common density functionals, BLYP (Figure 3 A) and HCTH predict excessively ordered second shells.[21] LEWIS trajectories show that the hydronium usually donates three strong hydrogen bonds, and rarely accepts a weak one, consistent with the Eigen picture.

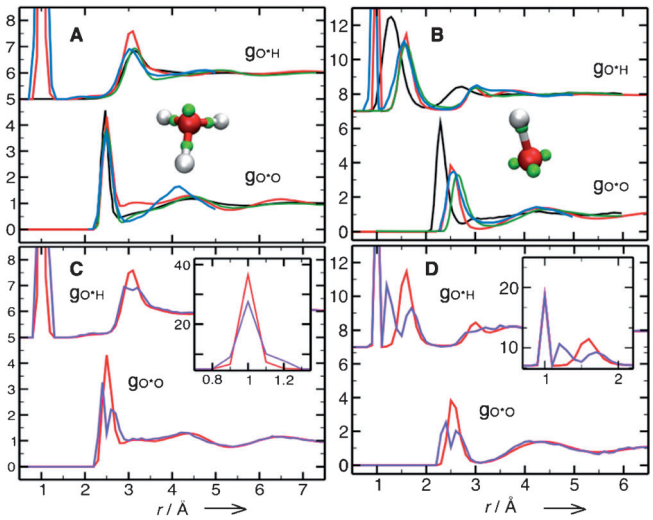

Figure 3. RDFs of solvated (A and C) hydronium and (B and D) hydroxide. Proton defect oxygen atoms are identified as O*. LEWIS results (——) are from moderately dilute (ca. 0.1 M) systems. Snapshots taken every 100 fs over 10 ns were used in (A) and (B). Snapshots taken every 10 fs over 1 ns were used in (C) and (D). In (A) results are also shown for BLYP (——, ca. 1.7 M),[27] MS-EVB3 (——, ca. 0.25 M),[2] and SPC/E-based empirical potential structure refinement of neutron scattering data (——, ca. 6.1 M).[20] In (B) results are also shown for BLYP (——, 1.5 M),[28] the empirical (nonreactive) charged ring model (——, 0.26 M),[24a] and SPC/E-based empirical potential structure refinement of neutron scattering data (——, ca. 4.6 M).[11] The comparison is complicated by the known concentration dependence of the solvation structure.[12] In (C) and (D), the LEWIS RDFs (——) are contrasted with RDFs obtained from the snapshots immediately before or after a proton transfer event (——). Insets show the full first peaks of g_{O^*H}.

For a proton hole, we deprotonated one water molecule among 500 (pH = ca. 13). Again, this is relatively dilute, with the advantage of minimizing overlap of the solvation shells. As with the excess proton, the proton hole is more mobile than water. Over 10 ns, the proton hole migrated with a diffusion constant, $D_{OH^-} = 0.15\ Å^2 ps^{-1}$ (Figure S2), which is intermediate between the $0.24\ Å^2 ps^{-1}$ value predicted for the excess proton and the $0.11\ Å^2 ps^{-1}$ value predicted for water.[14] This trend $(D_{H_3O^+} > D_{OH^-} > D_{H_2O})$ agrees with the notion that proton transfer barriers are lower in acidic solutions than in basic ones.[6,22] As shown in Figure 2, the predicted ratio $D_{OH^-}/D_{H_3O^+} = 0.15{:}0.24 = 0.63$ is reasonably close to the experimental ratio of 0.72. Again, ab initio MD predictions (for deuterated systems) depend strongly on the choice of density functional, with $D_{OH^-}/D_{H_3O^+}$ values of 5.88, 0.68, and 0.14, for PW91, BLYP, and HCTH, respectively (vs. the experimental ratio of 0.47 for deuterated systems).[8]

Structurally, LEWIS predicts traditional solvation in which the hydroxide oxygen usually accepts three hydrogen bonds (the Eigen analogue in Figure 1 C) and only rarely accepts four (Figure 1 E). Nevertheless, it predicts RDFs for proton holes (Figure 3 B) that are similar to those obtained from ab initio simulations that predict primarily four-fold coordination (Figure 1 E). This is evidently an instance of the well-recognized fact that "there may be several distinct structures that give equally reasonable agreement between

[diffraction] data and simulation."[23] The balance between three-fold versus four-fold hydroxide coordination (Figure 1C vs. E) can be influenced by the distribution of the lone pair electron density. Higher coordination numbers are observed in nonreactive models where hydroxide constructs have high azimuthal symmetries.[24] However, although the three-fold symmetry of LEWIS' lone pairs may bias the simulation against four-fold coordination, it remains that LEWIS predicts the correct trend of diffusion rates (Figure 2).

Trajectories for both the proton excess and the proton hole with 100 fs windows between snapshots (Figure S3) show a wide range of intervals between defect transfers, with some bursts and some relatively quiet periods. A closer examination also shows that proton transfers which occur after a short dwell time usually return the proton to the specific oxygen from which it came, whereas the proton transfers which occur after a long dwell time are usually to a new oxygen. This suggests that our 100 fs windows are likely to have missed some round trips. We therefore continued the simulations for an extra 1 ns with snapshots taken every 10 fs, a period comparable to that of a water-stretch vibration. Figure 4 shows quantitative analyses of the snapshots obtained at both intervals.

The distributions of observed dwell times in Figure 4A clearly show that they are governed by at least two distinct timescales, which is consistent with widely accepted models of proton transport mechanisms[25] in which the timescales reflect at least two prominent barriers, one that governs rapid (sub-picosecond) proton "rattling" between partners, and the other characterizing the slow (picosecond) hydrogen bond rearrangements.[26] The difference between the distributions from snapshots at 100 fs and 10 fs intervals clearly shows that the 100 fs windows did indeed miss many round trips. In fact, we cannot preclude the possibility that the 10 fs windows may have also missed some. Therefore, the timescales derived from the observed dwell times provide upper bounds on the timescales for true non-transfer intervals, although the 10 fs windows provide a tighter bound than the 100 fs windows. In Table S1, these bounds are compared with time constants reported from other studies.

Figure 4B shows how the return probability depends on the observed dwell time. The fact that the defects with the shortest dwell times essentially always (much more than 1/2 of the time) execute round trips indicates that rapid proton exchange is going on within a persistent special pair. To characterize these pairs, we made use of the snapshots acquired at 10 fs intervals, comparing RDFs calculated from the snapshots immediately before and after a proton transfer (the snapshots within 10 fs of observed events) with RDFs calculated from all the snapshots (Figure 3C and D). The results point to the Zundel ion in the case of hydronium and its analogue in the case of hydroxide. The conditional g_{O^*O} for the excess proton (Figure 3C) shows the same features seen in MS-EVB3 and HCTH studies.[26b] It suggests that proton transfer events involve one water in the first solvation shell moving closer to the hydronium while the rest become more distant. The conditional g_{O^*H} provides a complimentary view, consistent with one of the bonded protons having been pulled away from the hydronium while the others are drawn closer. The conditional RDFs for the proton hole (Figure 3D) show analogous features. The conditional g_{O^*O} is consistent with one water in the first solvation shell moving closer to the hydroxide while the others fall back. The conditional g_{O^*H} is consistent with a proton from the first solvation shell being drawn toward the hydroxide. Thus the hydronium and hydroxide scenarios are closely analogous, with Zundel-type species associated with proton transfer events in both cases.

Figure 4B also shows that defects with long dwell times (Eigen-type species) hardly ever (much less than 1/3 of the time) return to the oxygen from which they came. This suggests that the defect travels far enough during the extended non-transfer period to lose its original coterie, in spite of the fact that the vehicular diffusion is slower than that of water (Figure 4C). Between the two Eigen forms, the protonated one travels more slowly than the deprotonated one, which is consistent with the generally smaller diffusion coefficients of monovalent cations versus monovalent anions

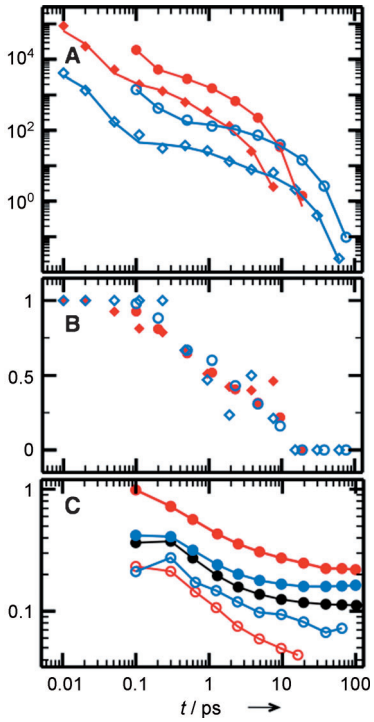

Figure 4. Defect dynamics for an excess proton (——) and a proton hole (——), as discerned from snapshots spaced by 100 fs (●/○/●/○) and 10 fs (◆/◇). A) The distributions of apparent dwell times (non-transfer intervals). The lines are triexponential fits ($m = 3$ in Eq. (S2)), with the time constants shown in Table S1. B) Fraction of transfers that return the proton defect to the oxygen atom from which it came vs. the length of the interval between the transfers. C) Comparison of vehicular diffusion (○/○) with total (vehicular plus structural) diffusion (●/●) over different intervals. Vehicular diffusion is calculated from the mean square displacements during non-transfer intervals. Total diffusion is calculated from all intervals of the same length (from the data in Figure S2), including for water (●). Rates (in units of $Å^2\,ps^{-1}$) are based on the end point of each interval and converge to the Einstein diffusion constant at long times. A–C) Bin lengths on the abscissa are logarithmic: 2^n(100 fs) for snapshots spaced by 100 fs, and 2^n(10 fs) for snapshots spaced by 10 fs.

of similar ionic radius.[29] The difference can be related to the time constants for convergence to the Einstein relation (Table S2). Random walks produce multinomial distributions that only converge to the Gaussians on which the Einstein relation depends after many steps. The convergence times show that it takes longer for hydronium to accumulate that many steps than hydroxide.

On the other hand, Figure 4C also shows that the two Zundel-type species (defects with short dwell times) have similar vehicular diffusion rates, within a factor of two of that of water. This suggests a similar degree of engagement of the two special pairs with the extended hydrogen bonding network. For all time intervals, the contribution of structural diffusion (proton hops) is much greater for the excess proton than for the proton hole, such that total defect diffusion is faster in acid on all time scales.

The overall picture that LEWIS paints for the proton transfer mechanism in the case of an excess proton is in close agreement with the "EZE" scenario of Markovitch et al., in which proton transfer depends on the transient conversion of the defect from the Eigen form to the Zundel form.[26b] The novel result is that the LEWIS picture for hydroxide is closely analogous. The special pair signature is the dichotomy between very high rates of proton return after short dwell times and very low rates of return after long dwell times (Figure 4B). This pattern may also be operative in ab initio and semi-empirical simulations of proton hole transport (based on visual inspection of Figure 4 in Tuckerman et al.[30] and Figure 12 in Ufimtsev et al.[31]). If the pattern is generally upheld by detailed quantitative analyses, then controversies over the mechanisms of defect transfer may have erred in placing their emphasis on the level of overall hydrogen bond coordination in solvation structures such as those in Figure 1, rather than focusing on the characteristics of the special pairs, how they are disrupted, and how new ones are formed.

In conclusion, key to a focus on the special pairs is the ability to run simulations that are sufficiently long to sample events to a high level of statistical confidence. In that respect, LEWIS is an excellent tool, simulating proton transfer in both acid and base, with trajectories of several nanoseconds, at ion concentrations of practical interest, with diffusion rates for proton defects relative to water that are more consistent with experiment than those rendered by much higher level theories, all without requiring any specific parameterization for aqueous hydronium or hydroxide.

Received: May 9, 2012
Revised: July 18, 2012
Published online: October 4, 2012

Keywords: diffusion · hydronium · hydroxide · proton transport · water chemistry

[1] a) N. Agmon, *Chem. Phys. Lett.* **1995**, *244*, 456 – 462; b) M. Tuckerman, K. Laasonen, M. Sprik, M. Parrinello, *J. Phys. Chem.* **1995**, *99*, 5749 – 5752; c) M. Tuckerman, K. Laasonen, M. Sprik, M. Parrinello, *J. Chem. Phys.* **1995**, *103*, 150 – 161.

[2] Y. Wu, H. Chen, F. Wang, F. Paesani, G. A. Voth, *J. Phys. Chem. B* **2008**, *112*, 7146 – 7146.

[3] a) C. C. M. Samson, W. Klopper, *J. Mol. Struct. THEOCHEM* **2002**, *586*, 201 – 208; b) M. E. Tuckerman, D. Marx, M. L. Klein, M. Parrinello, *Science* **1997**, *275*, 817 – 820.

[4] E. F. Aziz, N. Ottosson, M. Faubel, I. V. Hertel, B. Winter, *Nature* **2008**, *455*, 89 – 91.

[5] S. T. Roberts, P. B. Petersen, K. Ramasesha, A. Tokmakoff, I. S. Ufimtsev, T. J. Martinez, *Proc. Natl. Acad. Sci. USA* **2009**, *106*, 15154 – 15159.

[6] N. Agmon, *Chem. Phys. Lett.* **2000**, *319*, 247 – 252.

[7] D. Asthagiri, L. R. Pratt, J. D. Kress, M. A. Gomez, *Proc. Natl. Acad. Sci. USA* **2004**, *101*, 7229 – 7233.

[8] D. Marx, A. Chandra, M. E. Tuckerman, *Chem. Rev.* **2010**, *110*, 2174 – 2216.

[9] M. E. Tuckerman, D. Marx, M. Parrinello, *Nature* **2002**, *417*, 925 – 929.

[10] a) W. H. Robertson, E. G. Diken, E. A. Price, J. W. Shin, M. A. Johnson, *Science* **2003**, *299*, 1367 – 1372; b) C. Chaudhuri, Y. S. Wang, J. C. Jiang, Y. T. Lee, H. C. Chang, G. Niedner-Schatteburg, *Mol. Phys.* **2001**, *99*, 1161 – 1173.

[11] A. Botti, F. Bruni, S. Imberti, M. A. Ricci, A. K. Soper, *J. Mol. Liq.* **2005**, *117*, 81 – 84.

[12] B. Chen, J. M. Park, I. Ivanov, G. Tabacchi, M. L. Klein, M. Parrinello, *J. Am. Chem. Soc.* **2002**, *124*, 8534 – 8535.

[13] S. Kale, J. Herzfeld, S. Dai, M. Blank, *J. Biol. Phys.* **2012**, *38*, 49 – 60.

[14] S. Kale, J. Herzfeld, *J. Chem. Phys.* **2012**, *136*, 084109.

[15] H. L. Lemberg, F. H. Stillinger, *J. Chem. Phys.* **1975**, *62*, 1677 – 1690.

[16] C. J. Burnham, S. S. Xantheas, *J. Chem. Phys.* **2002**, *116*, 5115 – 5124.

[17] a) K. Krynicki, C. D. Green, D. W. Sawyer, *Faraday Discuss.* **1978**, *66*, 199 – 208; b) E. L. Littauer, K. C. Tsai, *Electrochim. Acta* **1979**, *24*, 351 – 355; c) N. K. Roberts, H. L. Northey, *J. Chem. Soc. Faraday Trans. 1* **1974**, *70*, 253 – 262.

[18] a) B. Halle, G. Karlstrom, *J. Chem. Soc. Faraday Trans. 2* **1983**, *79*, 1031 – 1046; b) E. H. Hardy, A. Zygar, M. D. Zeidler, M. Holz, F. D. Sacher, *J. Chem. Phys.* **2001**, *114*, 3174 – 3181.

[19] D. Marx, J. Hutter in *Modern Methods and Algorithms of Quantum Chemistry*, *Vol. 1* (Ed.: J. Grotendorst), John von Neumann Inst. of Computing, Julich, NIC Series, **2000**, pp. 301 – 449.

[20] A. Botti, F. Bruni, S. Imberti, M. A. Ricci, A. K. Soper, *J. Chem. Phys.* **2004**, *121*, 7840 – 7848.

[21] S. Izvekov, G. A. Voth, *J. Chem. Phys.* **2005**, *123*, 044505.

[22] Z. Luz, S. Meiboom, *J. Am. Chem. Soc.* **1964**, *86*, 4768 – 4769.

[23] S. E. McLain, S. Imberti, A. K. Soper, A. Botti, F. Bruni, M. A. Ricci, *Phys. Rev. B* **2006**, *74*, 094201.

[24] a) I. S. Ufimtsev, A. G. Kalinichev, T. J. Martinez, R. J. Kirkpatrick, *Chem. Phys. Lett.* **2007**, *442*, 128 – 133; b) X. Q. Sun, S. Yoo, S. S. Xantheas, L. X. Dang, *Chem. Phys. Lett.* **2009**, *481*, 9 – 16.

[25] N. Agmon, *Isr. J. Chem.* **1999**, *39*, 493 – 502.

[26] a) S. Woutersen, H. J. Bakker, *Phys. Rev. Lett.* **2006**, *96*, 138305; b) O. Markovitch, H. Chen, S. Izvekov, F. Paesani, G. A. Voth, N. Agmon, *J. Phys. Chem. B* **2008**, *112*, 9456 – 9466.

[27] M. E. Tuckerman, G. J. Martyna, *J. Phys. Chem. B* **2000**, *104*, 159 – 178.

[28] Z. W. Zhu, M. E. Tuckerman, *J. Phys. Chem. B* **2002**, *106*, 8009 – 8018.

[29] E. L. Cussler, *Diffusion: Mass Transfer in Fluid Systems*, 2nd ed., Cambridge University Press, Cambridge, UK, **1997**.

[30] M. E. Tuckerman, A. Chandra, D. Marx, *Acc. Chem. Res.* **2006**, *39*, 151 – 158.

[31] I. S. Ufimtsev, A. G. Kalinichev, T. J. Martinez, R. J. Kirkpatrick, *Phys. Chem. Chem. Phys.* **2009**, *11*, 9420 – 9430.

